



## Reflection response of the Parnaíba Basin from autocorrelation of seismic ambient noise recordings

Victória Maria de Almeida Santos Cedraz & Jordi Julià (DGef, UFRN), Martin Schimmel (I.C.T. “Jaume Almera”, CSIC), Verónica Rodríguez-Tribaldos & Nicky White (Bullard Laboratories, University of Cambridge)

Copyright 2017, SBGf - Sociedade Brasileira de Geofísica

This paper was prepared for presentation during the 15<sup>th</sup> International Congress of the Brazilian Geophysical Society held in Rio de Janeiro, Brazil, 31 July to 3 August, 2017.

Contents of this paper were reviewed by the Technical Committee of the 15<sup>th</sup> International Congress of the Brazilian Geophysical Society and do not necessarily represent any position of the SBGf, its officers or members. Electronic reproduction or storage of any part of this paper for commercial purposes without the written consent of the Brazilian Geophysical Society is prohibited.

### Abstract

We assess the ability of the autocorrelation of seismic ambient noise recordings in the recovery of the reflection response of the Parnaíba Basin of NE Brazil. The dataset was acquired by the Universidade Federal do Rio Grande do Norte and the University of Cambridge in 2015 under the Parnaíba Basin Analysis Project (PBAP), a multi-disciplinary and multi-institutional effort funded by BP Energy do Brasil. The dataset consists of 1 month of continuous ground motion data recorded at 10 short-period and 1 broadband stations in the central portion of the basin. Noise recordings were first split into 10 min-long windows, de-trended and tapered, and then band-pass filtered between 8 and 16 Hz to enhance high-frequency noise. Autocorrelation was then performed for all 10-min long windows, and the resulting time series were stacked with phase weighting to produce 31 daily autocorrelation functions (ACFs) for each site. Only the vertical component of ground motion was considered during analysis. The daily ACFs showed coherent wave-packets at lag times between 0.5 and 2.0 s, which were interpreted as topside reflections at intra-sedimentary discontinuities. Although denser networks would be advisable, we conclude that passive-source imaging of the Parnaíba basin with seismic ambient noise is feasible.

### Introduction

Reflected-wave interferometry relies on the recording of transient seismic signals from random wavefields located beneath recording stations. Under vertical incidence, the recordings contain the full transmission response, which includes the direct wave and multiple reverberations generated at seismic discontinuities located between the wavefields and the receiver. Analytical calculations show that the reflection response of the medium can be recovered from the autocorrelation function of the transmission response at a given receiver [e.g. Wapenaar et al., 2010], effectively mimicking the response that would be obtained had the wavefields originated at the free surface. The effectiveness of this approach was first demonstrated from autocorrelation of micro-earthquakes recorded at a monitoring network in Kilauea volcano, Hawaii [Daneshvar et al., 1995].

The use of ambient seismic noise in the development of autocorrelation functions for the recovery of the reflection

response, on the other hand, is more recent. Ito et al. [2012], for instance, computed ACFs from 300 days of continuous ambient seismic noise recordings at hundreds of seismic stations in Japan. By treating the ACFs as zero-offset seismic traces, they were able to recover the reflection response of the mantle wedge under Japan down to 150 km depth. Ambient noise autocorrelations were also used in the mapping of the crust-mantle boundary at single seismic stations [e.g. Tibuleac et al. 2012; Gorbатов et al., 2013; Taylor et al., 2016]. In this work, we investigate the use of ACFs from ambient seismic noise recordings to image seismic interfaces that separate the sedimentary sequences making up the Parnaíba basin of NE Brazil.

### Theoretical background

The use of ACFs in the retrieval of the reflection response of the medium under the recording station can be easily demonstrated for a simple layer-over-half space medium of uniform velocity. Following Wapenaar et al. (2010), we consider first the transmission response for an impulsive unit source located in the half-space portion of the medium. Such response includes the direct wave at  $t=t_0$ , and multiple reverberations between the free-surface and the bottom of the layer at multiples of the two-way travel-time across the layer ( $\Delta t$ ). Mathematically, this can be expressed as

$$T(t) = \tau \delta(t-t_0) - r\tau \delta(t-t_0-\Delta t) + r^2\tau \delta(t-t_0-2\Delta t) - \dots \quad (1)$$

where  $r$  is the reflection coefficient at the interface and  $\tau$  is the transmission coefficient (the reflection coefficient at the free surface is -1).

The ACF for this time series can be assessed analytically from  $T(t)*T(-t)$ , where  $*$  denotes convolution. Wapenaar et al. (2010) show that

$$T(t) * T(-t) = \delta(t) - R(t) - R(-t) \quad (2)$$

where

$$R(t) = r \delta(\Delta t) - r^2 \delta(2\Delta t) + r^3 \delta(3\Delta t) - \dots \quad (3)$$

Note that  $R(t)$  describes the reverberation of a plane wave from an impulsive source at the free-surface, co-located with the receiver. This is the reflection response of the medium, and eq. (2) demonstrates that such response can be recovered from the ACF of the transmission response.

Wapenaar et al. [2010] further demonstrate that eq. (3) holds for multi-layered media and multiple noise sources located in the half-space, after the delta function  $\delta(t)$  is replaced by the ensemble average of all (simultaneously acting) noise sources under the receiver.

## The dataset

The dataset utilized in this work was acquired under the umbrella of the Parnaíba Basin Analysis Project (PBAP), a multidisciplinary effort funded by BP Energy do Brasil that brings Brazilian and U.K. universities together to investigate the origin and evolution of this large cratonic basin of NE Brazil. Up to ten short-period stations were borrowed from the *Pool de Equipamentos Geofísicos do Brasil* (<http://www.pegbr.on.br>) and one broadband station was contributed by the University of Cambridge in the U.K. The ten short-period stations were symmetrically deployed along each side of the broadband station – located near the basin's depocenter – at ~10 km interstation distance, making a combined linear array of ~100 km in aperture (see Figure 1).

The short period stations were equipped with Sercel L4A-3D sensors – with flat response in velocity above 2 Hz – feeding RefTek 130 digitizers, and the broadband station consisted of a Güralp 3T sensor – with flat response in velocity between 120 s and 50 Hz – attached to a DM24 digitizer. All stations had GPS timekeeping and sampled continuously at 100 Hz. The short-period stations were deployed in 06/2015, while the broadband station was deployed two months later. Although all stations were in operation for over a year, we present here preliminary results based on 1 month of data (10/2015). Additional data will be incorporated into our analysis in the near future.

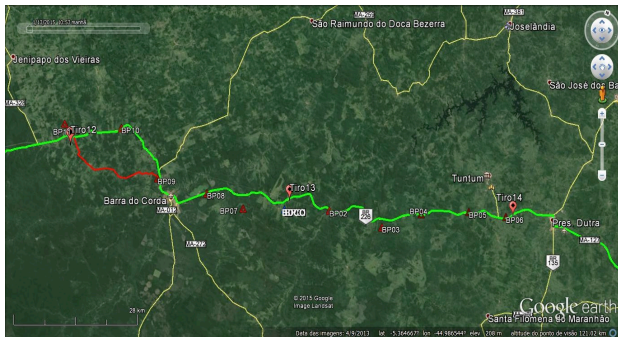


**Figure 1** – Station map showing the boundaries of the Parnaíba basin and the location of the seismic stations considered in this study.

## Developing ACFs from ambient seismic noise

As explained above, the development of the reflection response of a propagating medium from ambient seismic noise hinges on the computation of the ACFs at individual stations. To that end, daily recordings of ambient seismic noise were first compiled for a given station, and the daily recordings were then split into non-overlapping, 10-min long segments for analysis. Each segment was then demeaned, de-trended, and band-pass filtered between 8 and 16 Hz before autocorrelation. This bandwidth was chosen because it provided a reasonable balance between depth resolution (for sedimentary structure) and signal-to-noise ratio in the recovered reflection response. Autocorrelation was then performed on the 10-min long segments for lag times up to 5 s, and the resulting ACFs were finally stacked to produce daily ACFs for all the stations.

Two approaches were tested for the computation of the ACFs: (i) classical autocorrelation after normalization in the time (one-bit) and frequency (whitening) domains, similar to what is now routine processing for the recovery of surface-waves [e.g. Bensen et al., 2007]; and (ii) phase-autocorrelation [Schimmel, 1999] without normalization of the ambient seismic noise recordings [e.g. Schimmel et al., 2011]. Examples of daily (stacked) ACFs for Julian day 298 using each approach are displayed in Figure 2 for the broadband station BDCO. Careful inspection of the ACFs reveals that some signal is recovered at lag of 0.7 s and 1.0 s with the phase autocorrelation approach, while no signal is observed down to 5 s when using the classical autocorrelation with amplitude normalization. A superior performance of the phase autocorrelation was also noticed in the Ebro and Duero basins of Spain [Romero and Schimmel, 2017], and for Moho reflections in the North Anatolian Fault Zone [Taylor et al., 2016]. From the comparison, therefore, it is apparent that the best results will be obtained when using phase autocorrelation without normalization.

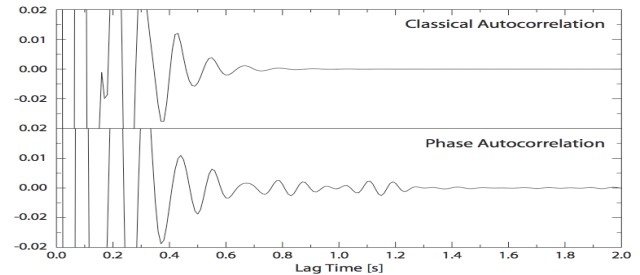


**Figure 2** – Daily autocorrelation functions (Julian day 298) for the station BDCO, obtained using the classical (top) and phase (bottom) autocorrelation approaches, respectively. Note the signal emerging at ~0.7 s and ~1.0 s in the phase autocorrelation trace.

Stacking to produce daily ACFs was implemented through the time-frequency domain phase-weighted stacking (tf-PWS) scheme of Schimmel and Gallart [2007]. tf-PWS uses the instantaneous phases of analytic signals to determine the coherence of the stack as function of time and frequency. This phase coherence is then used to attenuate incoherent noise from the linear stack. The approach was previously derived for the time domain [Schimmel and Paulssen, 1997] and has been introduced to ambient noise processing, together with the phase correlation, in Schimmel et al. [2011].

Nonetheless, stations BP03 and BP08 required additional 'cleaning' of the 10-min ACFs before being stacked to produce the daily ACFs. Figure 3a shows that the stacking of the 144 ACFs (10-min long) for day 276 at station BP08 has an apparent ringing behavior. Inspection of the amplitude spectra of the 10-min ACFs revealed that a resonant frequency at ~8 Hz dominates a large number of spectra (126 out of 144), with spurious spectral peaks being sometimes observed at higher frequencies (Figure 3b). Removing those 10-min long ACFs with resonant peaks from the daily stacks, nonetheless, eliminated the ringing behavior (Figure 3c). A similar behavior was observed at station BP03 (not shown), and a similar 'cleaning' process was thus applied to develop the daily ACFs for this station.

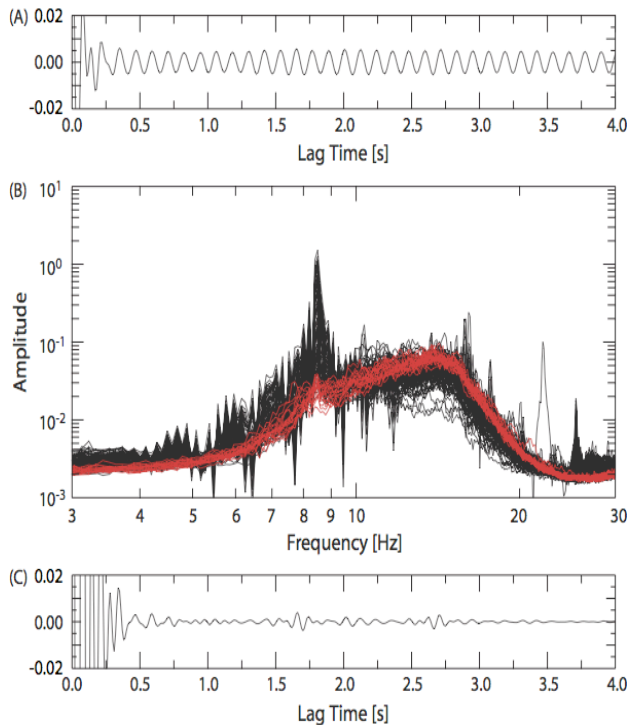


**Figure 3** – (a) Daily ACF for station BP08 (Julian day 276), obtained after stacking all 10-min long ACFs for that day. (b) Superposition of amplitude spectra for all 144 ACFs; note some spectra (black lines) have a marked resonant frequency at  $\sim 8$  Hz, while some others (red lines) do not; (c) Daily ACF for the same station, obtained after stacking those 10-min long ACFs with no resonant frequencies.

### Reflection response of the Parnaíba basin

A superposition of all daily ACFs for each of the stations considered in this study is shown in Figure 4. The ACFs display strong signals down to  $\sim 1.75$  s lag time, the lack of large-amplitude signal afterwards likely resulting from attenuation and scattering at high frequencies. Large “amplitudes” before 0.5 s are probably a superposition of side-lobes in the zero-lag autocorrelation and unresolved signals at short lag-times. Most of the stations display two wave-packets trailing the zero-lag signal (see Figure 4). They are best developed at stations BP06, BP03, and BP07, and have a very faint signature in the ACFs for stations BP02 and BP08. The second wave-packet in particular seems harder to identify at most of the stations.

According to the theoretical framework summarized before, the ACFs should be composed of upper-side reflections at seismic discontinuities. Moreover, as only the vertical component of the ambient seismic noise was utilized, those should be P-wave reflections. Considering the lag-times at which the wave-packets are observed are two-way travel-times, and assuming P-velocities of 2.0–3.0 km/s for the sediments, those could be preventively interpreted as P-wave reflections at depths in the 500–2625 m range. Moreover, considering basement depths of  $\sim 3000$  m for the basin [e.g. Daly et al., 2014], this would imply the retrieved wave-packets represent reflected P-wave energy at intra-sedimentary discontinuities.

Alternatively, the second wave-packet could be interpreted as reflected S-wave energy. This is demonstrated in Table 1, where the approximate travel times for the first ( $t_P$ ) and second ( $t_S$ ) wave-packets are listed, along with predicted depths to the (assumed) common interface. The table shows that for a P-velocity of 2.5 km/s and a  $V_P/V_S$  ratio of  $\sim 2.0$ , the agreement in predicted depths to the interface is remarkable. Leaking of S-wave energy into the vertical component could be explained, for instance, through scattering at small-scale heterogeneities in the propagating medium. Also, this alternative interpretation has the additional advantage of better explaining why the second wave-packet is generally weaker.

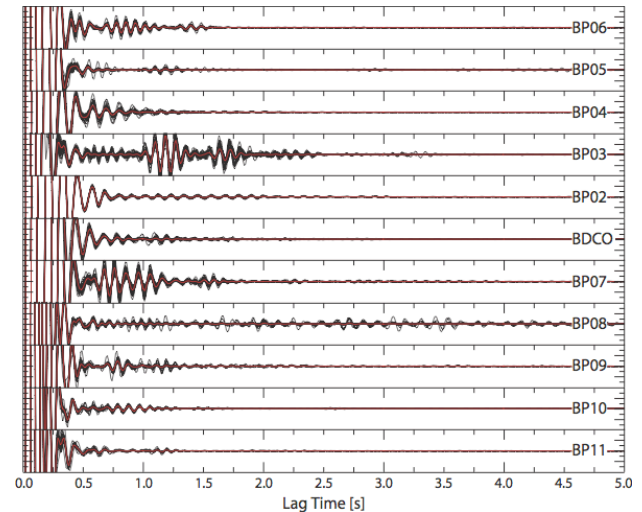


**Figure 4** – Daily ACFs (black lines) for the 11 seismic stations considered in this study. Note that stations are arranged by distance, from East (top) to West (bottom), according to location (see Figure 1). The monthly ACFs (stack of all daily ACFs) are superimposed in red.

**Table 1** - Predicted common interface depths

Station	P-wave		S-wave	
	twt (s)	h (m)	twt (s)	h(m)
BP06	0.75	0.94	1.38	0.86
BP05	0.63	0.78	1.25	0.78
BP03	1.13	1.41	1.63	1.02
BDCO	0.50	0.63	1.13	0.70
BP07	0.50	0.63	1.00	0.63
BP09	0.75	0.94	1.13	0.70
BP11	0.63	0.78	1.13	0.70

The next logical step in the development of the reflection response of the Parnaíba basin would be its migration into the depth domain. As noticed by Ito et al. [2002], the ACFs can be treated as zero-offset seismic traces recorded at the corresponding station. Such an exercise, however, would require a more accurate velocity model than that utilized in Table 1 for ray-tracing and, more importantly, a denser array of seismic stations to allow for a lateral continuous mapping of the sedimentary sequences. An added difficulty would be the presence of S-wave reflections in the ACFs, which would make the migrated images harder to interpret.

### Robustness of the recovered reflections

The robustness of the seismic reflections identified at each station can be assessed through inspection of the corresponding daily ACFs. This exercise is performed for station BP09 in Figure 5, where the 31 daily ACFs for this station are displayed along with their superposition and the monthly stack of the daily ACFs. The figures shows that the wave-packet at  $\sim 0.75$  s is consistently observed in the daily ACFs, suggesting that it is a robust feature in the reflection response for this station, while the wave-packet at  $\sim 1.1$  s is not. Note how this behavior results in the slower signal not emerging in the monthly ACF.

As the ACFs were developed from phase autocorrelation, their “amplitude” can be regarded as a measure of how much the ambient seismic noise at a given station is in phase with itself at a certain lag time. Realize that phase autocorrelation is thus explicitly amplitude-unbiased, and that changes in the strength of the noise should not have an impact on the “amplitude” of the recovered reflections. Amplitude variations among the daily ACFs are likely due to variations in the number (and position) of coherent noise sources over time. The decrease in autocorrelation (i.e. small amplitudes) is thus an indicator of the lack of coherent sources contributing to the seismic ambient noise during a particular time window (for which the ACF was developed). These considerations make apparent the need for sustained coherent noise sources during the recording time period in order to successfully recover body-wave reflections.

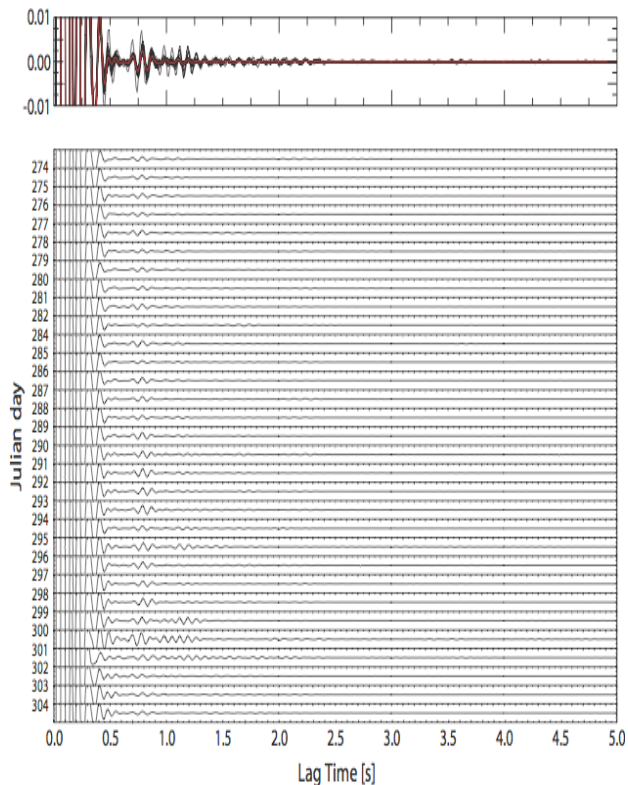


**Figure 5** – Daily ACFs for stations BP09 obtained from phase autocorrelation of seismic ambient noise recorded during July 2015. The red line is the stack of all daily ACFs (monthly ACF).

Variations in size among the monthly ACFs for the various stations (Figure 4) are harder to explain, as lateral variations in the elastic properties and density of the sediments might also be playing a role. Again, a denser deployment that allows for a more continuous mapping of lateral variations in depth and strength of the recovered reflections would be critical for confidently assessing the reliability of the recovery.

### Conclusions

We have developed high frequency (8-16 Hz) daily ACFs for 11 seismic stations in the Parnaíba Basin of NE Brazil, from phase autocorrelation of 1 month of (vertical) seismic ambient noise recordings. The daily ACFs show apparent wave-packets down to  $\sim 2.0$  s lag time, which are consistent with top-side reflections at intra-sedimentary discontinuities. Our results demonstrate the potential of ambient seismic noise recordings for the reconstruction of the reflection response of this basin. Denser networks with shorter interstation distances are nonetheless necessary for confidently assessing the recovery of the reflected body waves in the ACFs and to map seismic discontinuities in detail.

### Acknowledgments

Data acquisition and analysis was done under funding from BP Energy do Brasil (grant no FUNPEC-34/2014). VC thanks the *Programa de Recursos Humanos* of the *Agência Nacional do Petróleo, Gás e Biocombustíveis* for her research scholarship. JJ thanks the *Conselho Nacional de Desenvolvimento Científico e Tecnológico* (CNPq) for his research fellowship (CNPq, process no 304421/2015-4). MS acknowledges MISTERIOS (CGL2013-48601-C2-1-R).

### References

- BENSEN, G.D., M.H. RITZWOLLER, M.P. BARMIN, A.L. LEVSHIN, F. LIN, M.P. MOSCHETTI, N.M. SHAPIRO, Y. YANG.** 2007. Processing seismic ambient noise data to obtain reliable broad-band surface-wave dispersion measurements. *Geophys. J. Int.*, 169, 1239-1260.
- DANESHVAR, M.R., C.S. CLAY & M.K. SAVAGE.** 1995. Passive seismic imaging using microearthquakes. *Geophysics*, 60, 1178-1186.
- DALY, M.C., V. ANDRADE, C.A. BAROUSSE, R. COSTA, K. MCDOWELL, N. PIGGOTT & A.J. POOLE.** 2014. Brasiliano crustal structure and the tectonic setting of the Parnaíba basin of NE Brazil: Results of a deep seismic reflection profile. *Tectonics*, 33, doi:10.1002/2014TC003632.
- GORBATOV, A., E. SAYGIN & B.L.N. KENNETT.** 2013. Crustal properties from seismic station autocorrelograms, *Geophys. J. Int.*, 192, 861–870, doi: 10.1093/gji/ggs064.
- ITO, Y., K. SHIOMI, J. NAKAJIMA & R. HINO.** 2012.

Autocorrelation analysis of ambient noise in northeastern Japan subduction zone. *Tectonophysics*, 572-573, 38-46.

**SCHIMMEL, M. & H. PAULSEN.** 1997. Noise reduction and detection of weak, coherent signals through phase weighted stacks. *Geophys. J. Int.*, 130, 497-505.

**SCHIMMEL M., & J. GALLART.** 2007. Frequency-dependent phase coherence for noise suppression in seismic array data , *J. Geophys. Res.*, 112, B04303, doi:10.1029/2006JB004680

**SCHIMMEL, M., E. STUTZMANN & J. GALLART.** 2011. Using instantaneous phase coherence for signal extraction from ambient noise data at a local to a global scale, *Geophys. J. Int.*, 184, 494-506, doi: 10.1111/j.1365-246X.2010.04861.x

**TAYLOR, G., S. ROST & G. HOUSEMAN.** 2016. Crustal imaging across the North Anatolian Fault Zone from the autocorrelation of ambient seismic noise, *Geophys. Res. Lett.*, 43 , doi:10.1002/2016GL067715

**TIBULEAC, I.M. & D. VON SEGGERN.** 2012. Crust–mantle boundary reflectors in Nevada from ambient seismic noise autocorrelations, *Geophys. J. Int.*, 189, 493–500.

**WAPENAAR, K., D. DRAGANOV, R. SNIEDER, X. CAMPMAN & A. VERDEL.** 2010. Tutorial on seismic interferometry: Part 1 – Basic principles and applications, *Geophysics*, 75, 195-209.